Investigation of optical properties of CTBF0.3 using conventional solid state reaction method

Manali N. Shah[1], Pragati Parmar[2]
[1,2]*Department of Physics, Faculty of Science, Ganpat University, Mehsana–384012, Gujarat, India*

Abstract **- At present composite material have greater demand due to their unique properties so this paper is focused on introducing new composite material comprises of $CaTiO_3$ and $BiFeO_3$ using solid state reaction method. Bond presence in the produced composite is estimated using FTIR spectroscopy. The bond between Ti-O and Fe-O has been formed as a result of the obtained bond length values. Strong visible light absorption is detected using UV-visible spectroscopy, with an optical band gap value of 3.03 eV, suggesting the potential for photo-catalytic activities and its use in the production of optoelectronic devices.**

Index Terms **- $CaTiO_3$, $BiFeO_3$, FTIR , UV – visible spectroscopy.**

1.INTRODUCTION

Multiferroic materials like $BiMnO_3$, $BiFeO_3$, $YMnO_3$, Re (MnO_3), and $SrMnO_3$ have captured the interest of researchers in the current scientific era due to their critical applications in magnetic sensors, multiple state memories, data exhibiting storage devices, spintronics, and energy conversion, energy harvesting devices, high frequency devices, and magnetic controlled transducers. [1-4]. Strong coupling between two or more ferroic orderings, such as ferroelectricity, magnetism, or ferroelasticity, can be found in these materials, allowing one to tune the other by using an electric field or vice versa. [1-5]. The multiferroic $BiFeO_3$ (BFO) shows antiferromagnetism at 643 K (Neel temperature, T_N = 643 K) and ferroelectricity at room temperature (Curie temperature, TC = 1103 K) [6-7]. A $6S^2$ lone pair of the Bi^{3+} ion causes structural distortions that cause the ferroelectricity in BFO, whilst the canted Fe^{3+} spin structure's super exchange contacts cause weak ferromagnetism. [8-9]. BFO exhibits space-modulated spin periodicity of 62 nm together with scanted G-type antiferromagnetic ordering. [10-11]. Low resistivity, brittle magnetization, a significant amount of leakage current, and difficulty in single-phase preparation are some cons of BFO, nevertheless. [10-11].

Due to its fascinating features, such as electroceramic dielectricity, superconductivity, and ferroelectricity, materials with the perovskite structure ABO_3 ($CaTiO_3$) are frequently employed in both industry and research. The characteristics of perovskites can be easily altered by making minor modifications to the crystal structure and composition via doping. [12]. Due to its great qualities, such as its safety for human consumption, high dielectric properties, and permittivity, calcium titanate (CTO) has been studied in biomedical research as well as nanophosphor and photocatalytic applications [13-20].

2.SAMPLE PREPARATION AND EXPERIMENTAL METHODOLOGY

In this study, the solid-state reaction technique has been used to successfully synthesise (1-x) BFO + x CTO for x = 0.3. For 1 g of Bismuth Ferrite, the stoichiometric ratio is 0.744764 g Bismuth (III) Oxide (Bi_2O_3) and 0.255236 g Iron (III) Oxide. Similarly, for 1 g of Calcium Titanate, the ratio is 0.556183 g Calcium Carbonate ($CaCO_3$) and 0.443816 g Titanium dioxide (TiO_2). With the aid of an agate mortar and pestle, all of these powders were combined and ground. In order to ensure a homogenous mixture, the reactants were ground for eight hours. The next step involved adding fine powder to a crucible for a high-temperature reaction. In this instance, prepared powder samples were heated in a box-style muffle furnace for 24 hours at 700º C. Using the correct stoichiometry, 0.1570 g of $CaTiO_3$ and 0.8430 g of $BiFeO_3$ were further combined and ground to create polycrystalline material of CTBF0.3, which was then used to construct the composite for x = 0.3. The ease of use and high-volume production are two benefits of the solid-state reaction process. The entire

experimental process for creating CTBF0.3. temperature is shown in Figure 1.

3.RESULT AND DISCUSSION

In this section, results of FTIR spectroscopy and UV visible spectroscopy are discussed in detail with band gap analysis and other optical parameters.

3.1 FTIR Spectroscopy: (Fourier Transform Infrared Spectroscopy)

The 500 cm^{-1} to 4000 cm^{-1} range of the FTIR test was performed at room temperature. Figure 2 displays the composite $Bi_{0.7}Ca_{0.3}FeO_3$'s FTIR spectrum. The peaks at 552 cm^{-1} in the $Bi_{0.7}Ca_{0.3}FeO_3$ crystallites were assigned to the mode of stretching vibrations along the Fe-O axis and the mode of the Fe-O bending vibration, which are characteristics of the octahedral FeO_6 groups in the perovskite compounds, as is well known. The bands between 700 and 500 cm^{-1} were also primarily attributed to the formation of metal oxides [2, 21]. The existence of the metal-oxygen band is evidence that the perovskite structure has formed [22]. Iron oxide vibration bands correlate to 552 cm^{-1} peak values. The BiO_6 octahedral unit is represented by the absorption band at 674 cm^{-1} and 814 cm^{-1}. Titanate-based materials can be identified by their prominent absorption bands below 1000 cm^{-1}, which are present in the transmittance FTIR spectra at 814 cm^{-1}, 674 cm^{-1}, and 552 cm^{-1}. These bands are connected to the titanium cation and the stretching vibration of Ti-O between 700 cm^{-1} and 500 cm^{-1}. The presence of trapped nitrates and carbonate group during the exposure of the sample to air caused the peak between 1500 cm^{-1} and 1200 cm^{-1}.Value of force constant k can be determined via equation $f = \frac{1}{2\pi}\sqrt{\frac{k}{\mu}}$. Using the formula $c = \lambda f$, the vibrational frequency (f) for each of the prepared samples is computed. Effective mass of the Fe - O bond is obtained by: $\mu_{eff} = \frac{\mu_O * \mu_{Fe}}{\mu_O + \mu_{Fe}}$

where,

$c = velocity\ of\ light = 3 * 10^8 m/s$

$\lambda = wavelength,$

$which\ is\ reciprocal\ of\ wave\ number\ of\ a\ given\ samp$

Since the mass of elements (Fe, O, and Ti) is in atomic mass unit, it is converted to kilogrammes using the conversion relation $1amu = 1.66 * 10^{-27}\ kg$ [23]. The formula $k = \frac{17}{r^3}$ can be used to link the force constant to the typical Fe-O bond Length.

Figure 1: Experimental procedure for the formation of CTBF0.3

Thus, the samples' bond length (r) has been calculated using this equation. Below are the calculated values for vibration frequency, effective mass, bond length, and force constant.

$Concentration(x) = 0.3$

$Wave\ number\ (\upsilon) = 552\ cm^{-1}$

$Effective\ mass\ (\mu) = 2.0422 \times 10^{-27}\ kg$

$Force\ constant\ (k) = 2.2087\ N/cm$

$Frequency\ of\ vibration\ (f) = 1.656 \times 10^{13} Hz$

$Bond\ length\ (r) = 1.9744\ Å,$

$Bonding = Fe - O + Ti - O$

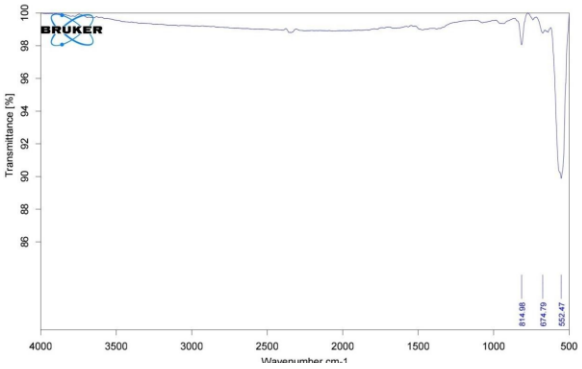

Figure 2 : FTIR spectrum of CTBF0.3

3.2 Ultraviolet Visible spectroscopy

UV- Vis spectroscopy was used to examine how the CTO substitution affected the optical characteristics of BFO. Figure 3 displays the CTBF0.3 absorption spectra in the 200–800 nm wavelength range. The samples' absorption falls within this range and exhibits high absorption between 300 and 600 nm. Using the samples' absorption profiles and the well-known Tauc's relation for the direct band gap [24–26], the band gaps of all the samples were determined via $(\alpha h\vartheta^2) = A\left(h\vartheta - E_g\right)$where,α,υ, h, A, and Eg are, respectively, the absorption coefficient, the frequency of light, the Planck constant, the constant of proportionality, and the band gap. Plotting $(\alpha h\vartheta^2) vs\ h\upsilon$ (photon energy) yielded the band gap of CTBF0.3, as seen in Figure 3b. The band gap value is obtained by projecting the most linear section of the $(\alpha h\vartheta^2)\ vs\ h\upsilon$ plot up to the point α = 0. 3.03 eV are the calculated band gap values for CTBF0.3. The oxygen vacancies are another element that could have an impact on the band gap.

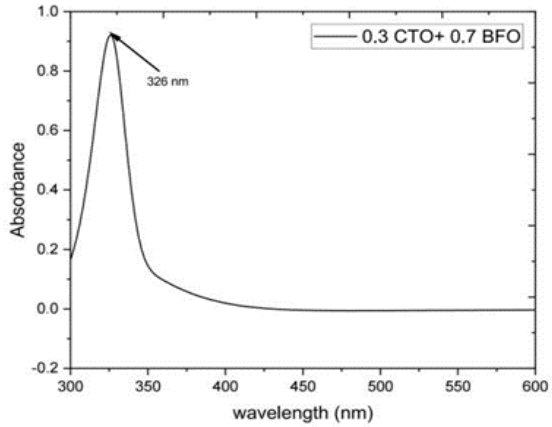

Figure: 3 (a) UV - Vis absorption spectra

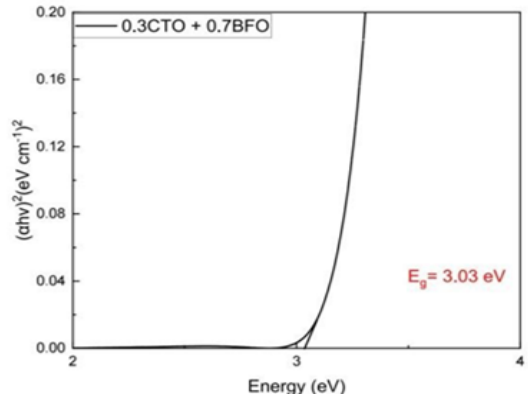

Figure: 3 (b) Tauc's plots to determine the band gap

4.CONCLUSION

We have successfully synthesized the polycrystalline material CTBF0.3 using solid state reaction method. FTIR results confirm the Fe – O bond and U.V. visible shows that material is wide band gap semiconducting material.

5.ACKNOWLEDGEMENT

We are thankful to Department of Chemistry, Mehsana Urban Institute of Sciences, Ganpat University for providing the experimental facility.

REFERENCE

[1] Ma, J., Hu, J., Li, Z., & Nan, C. W. (2011). Recent progress in multiferroic magnetoelectric composites: from bulk to thin films. Advanced materials, 23(9), 1062-1087.

[2] Kumar, V., & Singh, S. (2018). Optical and magnetic properties of (1-x) BiFeO3-xCaTiO3 nanoparticles. Journal of Alloys and Compounds, 732, 350-357.

[3] Khan, B., Kumar, A., Yadav, P., Singh, G., Kumar, U., Kumar, A., & Singh, M. K. (2021). Structural, dielectric, magnetic and magneto-dielectric properties of (1− x) BiFeO3–(x) CaTiO3 composites. Journal of Materials Science: Materials in Electronics, 32(13), 18012-18027.

[4] Eerenstein, W., Mathur, N. D., & Scott, J. F. (2006). Multiferroic and magnetoelectric materials. nature, 442(7104), 759-765.

[5] Spaldin, N. A., Cheong, S. W., & Ramesh, R. (2010). Multiferroics: Past, present, and future. Phys. Today, 63(10), 38-43.

[6] Zhang, Q., Zhu, X., Xu, Y., Gao, H., Xiao, Y., Liang, D.,& Xiao, D. (2013). Effect of La3+ substitution on the phase transitions, microstructure and electrical properties of Bi1− xLaxFeO3 ceramics. Journal of Alloys and Compounds, 546, 57-62.

[7] Ederer, C., & Spaldin, N. A. (2005). Weak ferromagnetism and magnetoelectric coupling in bismuth ferrite. Physical Review B, 71(6), 060401.

[8] Wang, Q. Q., Wang, Z., Liu, X. Q., & Chen, X. M. (2012). Improved structure stability and multiferroic characteristics in CaTiO3-modified

BiFeO3 ceramics. Journal of the American Ceramic Society, 95(2), 670-675.

[9] Ma, Y., & Chen, X. M. (2009). Enhanced multiferroic characteristics in NaNbO3-modified BiFeO3 ceramics. Journal of Applied Physics, 105(5), 054107.

[10] Khomchenko, V. A., Kiselev, D. A., Vieira, J. M., Kholkin, A. L., Sá, M. A., & Pogorelov, Y. G. (2007). Synthesis and multiferroic properties of bi 0.8 a 0.2 fe o 3 (a= ca, sr, pb) ceramics. Applied physics letters, 90(24), 242901.

[11] Yan, J., Gomi, M., Yokota, T., & Song, H. (2013). Phase transition and huge ferroelectric polarization observed in BiFe1− xGaxO3 thin films. Applied Physics Letters, 102(22), 222906.

[12] Rai, R., Valente, M. A., Bdikin, I., Kholkin, A. L., & Sharma, S. (2013). Enhanced ferroelectric and magnetic properties of perovskite structured Bi1− x− yGdxLayFe1− yTiyO3 magnetoelectric ceramics. Journal of Physics and Chemistry of Solids, 74(7), 905-912.

[13] Bhalla, A. S., Guo, R., & Roy, R. (2000). The perovskite structure—a review of its role in ceramic science and technology. Materials research innovations, 4(1), 3-26.

[14] Naganuma, H., Miura, J., & Okamura, S. (2008). Ferroelectric, electrical and magnetic properties of Cr, Mn, Co, Ni, Cu added polycrystalline Bi FeO3 films. Applied Physics Letters, 93(5), 052901.

[15] Wang, T. H., Tu, C. S., Ding, Y., Lin, T. C., Ku, C. S., Yang, W. C., & Lee, H. Y. (2011). Phase transition and ferroelectric properties of xBiFeO3–(1− x)BaTiO3 ceramics. Current Applied Physics, 11(3), S240-S243.

[16] Vura, S., Kumar, P. A., Senyshyn, A., & Ranjan, R. (2014). Magneto-structural study of the multiferroic BiFeO3–SrTiO3. Journal of magnetism and magnetic materials, 365, 76-82.

[17] Mishra, V., Kumar, V., & Singh, S. (2016). Structural, optical and magnetic properties of multiferroic (1− x) BiFeO3xPbTiO3 nanoparticles. Journal of Alloys and Compounds, 683, 133-138.

[18] Lahmar, A., Habouti, S., Solterbeck, C. H., Es-Souni, M., & Elouadi, B. (2009). Correlation between structure, dielectric, and ferroelectric properties in BiFeO3–LaMnO3 solid solution thin films. Journal of Applied Physics, 105(1), 014111.

[19] Patel, J. P., Senyshyn, A., Fuess, H., & Pandey, D. (2013). Evidence for weak ferromagnetism, isostructural phase transition, and linear magnetoelectric coupling in the multiferroic Bi 0.8 Pb 0.2 Fe 0.9 Nb 0.1 O 3 solid solution. Physical Review B, 88(10), 104108.

[20] Troyanchuk, I. O., Karpinsky, D. V., Bushinskii, M. V., Prokhnenko, O., Kopcevicz, M., Szymczak, R., & Pietosa, J. (2008). Crystal structure and properties of Bi1− x Ca x FeO3 and Bi1− x Cax FeO1− xTi x O3 solid solutions. Journal of Experimental and Theoretical Physics, 107(1), 83-89.

[21] Qing Wang, Q., Jian Zhao, H., & Ming Chen, X. (2012). Low-temperature dielectric behavior of BiFeO3-modified CaTiO3 incipient ferroelectric ceramics.

[22] Kazhugasalamoorthy, S., Jegatheesan, P., Mohandoss, R., Giridharan, N. V., Karthikeyan, B., Joseyphus, R. J., & Dhanuskodi, S. (2010). Investigations on the properties of pure and rare earth modified bismuth ferrite ceramics. Journal of alloys and compounds, 493(1-2), 569-572.

[23] Shah, M. N., Patel, N. H., Shah, D. D., & Mehta, P. K. (2021). FTIR: Important tool to investigate the chemical bond formation in the polycrystalline xBaTiO3–(1-x) BiFeO3. Materials Today: Proceedings, 47, 616-620.

[24] Mocherla, P. S., Karthik, C., Ubic, R. N. A. R., Ramachandra Rao, M. S., & Sudakar, C. (2013). Tunable bandgap in BiFeO3 nanoparticles: the role of microstrain and oxygen defects. Applied Physics Letters, 103(2), 022910.

[25] Li, S., Lin, Y. H., Zhang, B. P., Wang, Y., & Nan, C. W. (2010). Controlled fabrication of BiFeO3 uniform microcrystals and their magnetic and photocatalytic behaviors. The Journal of Physical Chemistry C, 114(7), 2903-2908.

[26] Wu, X., Kuang, D., Yao, L., Yang, S., & Zhang, Y. (2017). The structural, optical, ferroelectric properties of (1-x) BiFeO3-xCaTiO3 thin films by a sol–gel method. Journal of Materials Science: Materials in Electronics, 28(1), 493-500.